American Mineralogist, Volume 76, pages 230–240, 1991

CH_4-rich inclusions from quartz veins in the Valley-and-Ridge province and the anthracite fields of the Pennsylvania Appalachians

H. J. Kisch
Department of Geology and Mineralogy, Ben-Gurion University of the Negev, P.O.B. 653, Beer Sheva 84 105, Israel
A. M. van den Kerkhof
Institut für Geologie und Dynamik der Lithosphäre, Goldschmidtstraße 3, 3400 Göttingen, Germany

Abstract

The temperatures and pressures of diagenesis and very low-grade metamorphism of the Palaeozoic formations of the Valley-and-Ridge province in the central Appalachians are revealed by analyzing their fluid inclusions. Samples from two areas were studied and compared: (1) the Silurian and Devonian Delaware Water Gap area and (2) the anthracite region of eastern Pennsylvania. Gaseous CH_4-CO_2 and aqueous ($\pm CH_4$) inclusions were studied by microthermometry; gas compositions were measured by Raman analysis. The two fluids are thought to have been immiscible, saturated fluids. The isochores calculated for both types of inclusions indicate fluid trapping *P-T* conditions of about 195–245 °C, 0.8–1.3 kbar for the anthracite region, but higher pressures (1.3–1.9 kbar at 180–230 °C, and possibly as much as 2.2–2.5 kbar) for the Delaware Water Gap area. The pressure difference reflects the relative stratigraphic position of the rock formations, and a higher thermal gradient for the anthracite region. The fluid trapping temperatures and pressures are consistent with conodont alteration indices (CAI), illite crystallinities, the anthracite rank, slaty cleavage development, and the stability of pyrophyllite.

Introduction

The folded Palaeozoic terranes of the Great Valley and Valley-and-Ridge provinces of the central Appalachians are traditionally regarded as unmetamorphosed. However, their very low-grade metamorphism is evident from conodont alteration studies (Epstein et al., 1977; Harris et al., 1978), and from anthracite rank and the occurrence of pyrophyllite in underclays (Hosterman et al., 1970) in the Pennsylvanian. As a further test of metamorphic *P-T* conditions, we analyzed fluid inclusions in quartz veins from two different areas (Fig. 1):

1. The Delaware Water Gap–Stroudsburg area, northwestern New Jersey and eastern Pennsylvania whose rock units include: (a) the Martinsburg Formation (Ordovician Taconic flysch) of the northwestern margin of the Great Valley. The prominent slaty cleavage of this unit has been the subject of extensive studies by Maxwell (1962) and subsequent workers (e.g., Epstein and Epstein, 1969; Groshong, 1976; Beutner, 1978); (b) the Shawangunk (Lower and Middle Silurian), Helderburg and Oriskany (Lower Devonian), and Marcellus (Middle Devonian) Formations overlying the Taconic unconformity.

2. The Pennsylvanian coal measures of the anthracite region of eastern Pennsylvania, situated some 50 to 100 km to the northwest and southwest of the former area.

The rocks mainly consist of metasediments (shales, mudstones, etc.) crosscut by quartz veins. In addition to aqueous inclusions, many of these quartz veins contain methane-rich fluid inclusions that were studied in order to obtain information on the rock-forming pressures and burial depth.

Deformation and very low-grade metamorphism

Slaty cleavage in the Martinsburg Formation

The closely spaced slaty cleavage at the Delaware Water Gap has been ascribed by some authors to deformation during the Late-Ordovician Taconic deformation (e.g., Maxwell, 1962; Beutner and Diegel, 1985), while others (e.g., Epstein and Epstein, 1969; Drake, 1969) have considered it to result mainly from the Late-Paleozoic Alleghenian deformation that has deformed the Silurian-Pennsylvanian sequence of the northwesterly adjoining Valley-and-Ridge province.

Holeywell and Tullis (1975) showed that the development of slaty cleavage in the Martinsburg Formation in the nearby Lehigh Gap near its contact with the overlying Silurian Shawangunk Formation mainly involved mica solution and recrystallization.

Groshong (1976) and Beutner (1978) showed that the slaty cleavage southeast of the Delaware Water Gap formed largely by pressure solution and redepositing of quartz and phyllosilicates, and that no rotation of the platy minerals took place during the cleavage formation (see also Beutner and Diegel, 1985). Lee et al. (1986) suggested that these processes were syntectonic and involved transitions from imperfect metastable toward ordered stable phases. They estimated the sediment thick-

0003–004X/91/0102–0230$02.00

ness above the Martinsburg Formation at the Lehigh Gap at the time of the Alleghenian orogeny as approximately 7.5 km (or $P_{lith.}$ = 2 kbar), and calculated the temperature as 225 ± 75 °C (assuming an average geothermal gradient of 30 ± 10 °C/km). The Ordovician of the Great Valley of easternmost Pennsylvania lies in the area wherein the conodont alteration index (CAI) = 4.5–5, as described by Harris et al. (1978) and estimated by those authors to represent a temperature range of 250–300 °C to 350–400 °C for heating durations of >50 to 1 Ma.

Very low-grade metamorphism in the Silurian-Pennsylvanian

Very low-grade metamorphism in the Silurian-Pennsylvanian sequence is indicated by several lines of evidence: (1) The predominantly anthracitic rank of the Pennsylvanian coals in the larger synclines (the Pennsylvania anthracite fields), semianthracitic ranks being found only in the westernmost extensions of the western middle and southern fields. (2) The widespread occurrence of pyrophyllite in the underclays of the anthracites (Hosterman et al., 1970); recently, Juster et al. (1987) have reported on the widespread occurrence of ammonium illite in mudrocks of the northeast Pennsylvania anthracite and semianthracite fields, occurring together with illite, ± paragonite, ± pyrophyllite (two or all of these three phyllosilicates in all except one sample), chlorite, and in many samples of kaolinite. (3) The high CAI of predominantly four to five in the Silurian through Middle Devonian carbonate rocks (Harris et al., 1978); such CAI values correspond with anthracite coal ranks with reflectance R_0 = 1.95–3.6 to >3.6% and with temperatures of 190–300 °C to 300–400 °C for heating durations of >50 to 1 Ma (Epstein et al., 1977, Fig. 11; Harris et al., 1978, Table 1).

Grade of metamorphism: Illite crystallinities

The grades of incipient metamorphism were further established by the illite crystallinity method (Kubler, 1967, 1968) using the preparation and instrumental settings described by Kisch (1980a, 1980b). At these instrumental settings the limits of the anchimetamorphic zone corresponding to Kubler's (1967) boundary values of 0.42 and 0.25°Δ2θ are 0.38 and 0.21°Δ2θ. For the two terranes studied these are as follows (all values are from Mg-saturated 2 μm fractions):

1. (a) Anchimetamorphic to epimetamorphic: mean 0.21°Δ2θ (five samples—range 0.16 to 0.25°Δ2θ). Somewhat lower-grade illite sharpness-ratio ($I_{10Å}/I_{10.5Å}$ after Weaver, 1961) values of 5–10 are reported by Lee et al. (1986, Fig. 3) from the mudstone to slate transition in the Martinsburg Formation of the Lehigh Gap (some 40 km southwest of the Delaware Water Gap: see Fig. 1). From the same section Kisch has measured equivalent medium- and high-grade anchimetamorphic illite crystallinities of 0.24–0.31°Δ2θ (in Wintsch et al., in preparation). (b) Medium to high-grade anchimetamorphic in the Silurian and Lower Devonian: mean 0.27°Δ2θ (eight samples—range 0.23 to 0.30°Δ2θ); low- to medium-grade anchimetamorphic in the Middle Devonian (Marcellus Formation), 0.31–0.36°Δ2θ (two samples). These data have been earlier summarized by Kisch (1987, Table 7.3).

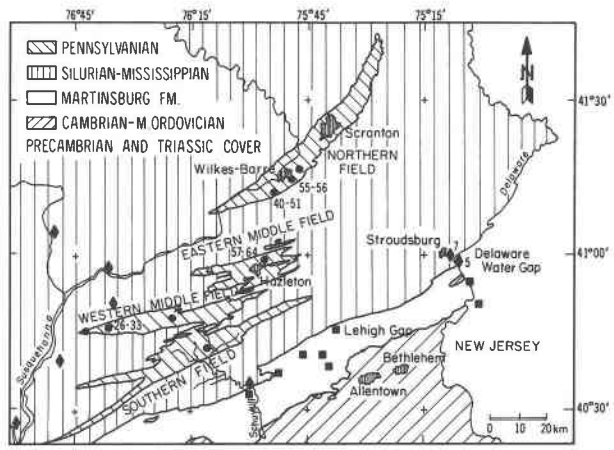

Fig. 1. Geological sketch map of central eastern Pennsylvania. All localities from which illite crystallinity determinations have been made are indicated (squares: localities from the Martinsburg Formation; diamonds: Silurian-Mississippian; circles: Pennsylvanian); sample numbers are given only for localities from which methane-rich fluid inclusions have been studied.

2. Diagenetic: range 0.40 to 0.80°Δ2θ (19 samples—seven from the northern, six from the western middle, two from the eastern middle, and four from the southern anthracite field). In many of the samples the 10 Å peaks are broadened because of the presence of pyrophyllite (Hosterman et al., 1970) and the 10.35 Å peaks of ammonium illite (Juster et al., 1987). Of the eight samples entirely free of these minerals, six have 10 Å peak widths between 0.40 and 0.61°Δ2θ. One of the two exceptions with broader peaks is an underclay from the westernmost extension of the western middle field where the coal ranks are semianthracitic, whereas all other samples are taken from anthracite-rank areas. The other exception is from a vermiculite-bearing green claystone from the southern field. Juster et al. (1987) report illite crystallinities of 0.3–0.45°Δ2θ from the anthracite areas, but no details are given on instrumental settings.

Fluid inclusions in the quartz veins

The quartz veins are up to 2 cm wide and commonly crosscut the bedding; they also crosscut the slaty cleavage, where present, as in some of the lower Palaeozoic rocks. The fluid inclusions occur in clusters or have an isolated occurrence (i.e., do not occur along planes).

The CH_4-CO_2 fluids, most probably of organic origin, were found only in the quartz veins from terranes 1b and 2; none were found in those from the Martinsburg slates (1a). These inclusions show a subhedral to euhedral negative crystal shape. Necking-down or stretching textures were observed locally. Inclusions of different gas composition and molar volume cannot be distinguished on

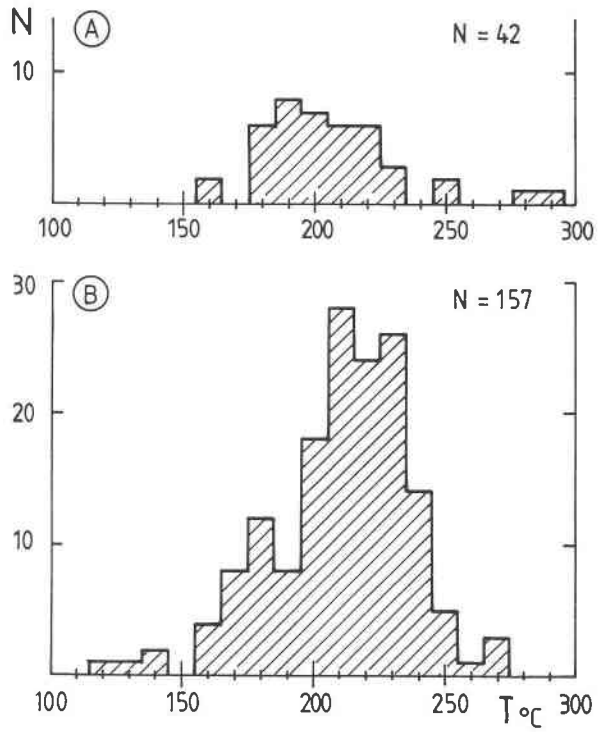

Fig. 2. Histograms of homogenization temperatures of aqueous inclusions in quartz veins that also contain methane-rich inclusions: (A) Silurian and lower Devonian of the Delaware Water Gap (samples Ap79-5C and Ap79-7B) (B) Pennsylvanian of the anthracite region (six samples).

textural grounds as they all have a similar appearance. The size is generally between 20 and 40 μm, but much larger inclusions, up to 90 μm in size, were found in a few samples from the anthracite fields.

The quartz veins contain two types of fluid inclusions: aqueous and methane-rich. The aqueous fluid inclusions generally have a small gas bubble at room temperature, and homogenize into the liquid phase at temperatures ($T_{h,aq.}$) ranging from 150 to >290 °C (predominantly 180–230 °C) in the samples from the Silurian and Devonian, and from 120 to 275 °C (predominantly 195–245 °C) in the samples from the Pennsylvania anthracite fields. Histograms of the homogenization temperatures measured in the two areas studied are shown as Figures 2A and 2B. In the samples from the Silurian and Devonian, several inclusions decrepitated before homogenization upon heating at temperatures between 160 and 250 °C.

The melting temperatures of the ice ($T_{m,aq.}$) are higher than about −8 °C, indicating low salt contents of less than 12 wt% NaCl-equivalent; no correlation between $T_{h,aq.}$ and $T_{m,aq.}$ was found. In some distorted parts, large halite crystals could be incidentally observed at room temperature in aqueous inclusions (>25 wt% NaCl). Their homogenization temperatures (260–340 °C) are mostly in the higher $T_{h,aq.}$ range and about equal to $T_{h,aq.}$ for the directly associated H_2O inclusions. Neither can these inclusions be clearly distinguished from the other H_2O inclusions on textural grounds. Clathrates in H_2O-CH_4 inclusions, if formed during freezing experiments, were not observed, probably because of the small size of the vapor bubble.

The methane-rich inclusions contain a single-phase fluid at room temperature. In most inclusions both a gas bubble and solid CO_2 appear upon cooling to temperatures below −70 °C. Upon subsequent heating, these gas and solid phases disappear—predominantly in this order, but in a subordinate population in the opposite order—by homogenization into the liquid phase (see below).

Both types of inclusions occur as isolated inclusions and clusters, usually with a somewhat elongated shape, and have the appearance of being primary. Aqueous and methane-rich inclusions of this type often occur in close proximity, and even in the same quartz crystals. Areas with primary-like fluid inclusions are separated by planar zones containing fluid inclusions that are evidently later in origin, formed either by decrepitation of the primary fluid inclusions or by trapping of fluids on healed cracks. The presence of extremely irregular shapes of empty cavities, which possibly contain very low-density gas, may be evidence for local strong decrepitation.

The primary aspects and the close proximity of the aqueous and methane-rich inclusions suggest trapping of two immiscible fluids (e.g., Pichavant et al., 1982), i.e., the methane-rich fluid must have been saturated with H_2O, and the aqueous fluid with CH_4, at the time of trapping. High homogenization temperatures of some of the aqueous inclusions (>240 °C in the Silurian and lower Devonian of the Delaware Water Gap) probably represent heterogeneous trapping.

Phase transitions in methane-rich fluid inclusions

Phase transitions were studied at temperatures between −180 and +35 °C with a Chaixmeca heating-freezing stage (Poty et al., 1976) cooled by liquid N_2. Calibration was carried out by using the melting temperatures of methylcyclopentane (−142 °C), n-heptane (−90.6 °C), pure CO_2 (−56.6 °C), and H_2O (0 °C) and of several other compounds above room temperature.

The classification of phase transitions upon warming from −180 °C—the minimum temperature obtainable when cooling with liquid N_2—is that proposed by van den Kerkhof (1988a, 1990) and shown as Table 1.

It was found that the inclusions contain three phases at temperatures below about −100 °C, namely a liquid phase (L), a vapor phase (V), and solid CO_2 (S). Complete solidification of the inclusions is not possible by cooling our stage with liquid N_2. On subsequent warming, most inclusions show homogenization of liquid and vapor before the melting of the solid phase, some other inclusions show melting followed by homogenization.

Sublimation is defined here as the direct transition from

TABLE 1. Phase transitions on warming CO_2-CH_4-N_2 inclusions at constant volume

	Phase transition	Denotation
Incipient melting*	$S + V \rightarrow S + L + V$	T_i L
	$S + L \rightarrow S + L + V$	T_i V
(Final) melting	$S + L + V \rightarrow L + V$	T_m
Partial homogenization**	$S + L + V \rightarrow S + V$	T_{hs} V
	$S + L + V \rightarrow S + L$	T_{hs} L
Homogenization/metastable homogenization	$L + V \rightarrow V$	T_h V/T_{hm} V
	$L + V \rightarrow L$	T_h L/T_{hm} L
Sublimation (evaporation)	$S + V \rightarrow V$	T_s V
Sublimation (dissolution)	$S + L \rightarrow L$	T_s L
Eutectic melting	$S_1 + S_2 + V \rightarrow S_1 + L + V$	T_e

* In earlier works of the author T_i L was denoted as T_i V, T_i V as T_i L. The modification was suggested by E. Roedder (personal communication).
** Homogenization of liquid and vapor in the presence of solid CO_2 (after van den Kerkhof, 1988a; 1990).

solid to vapor or from solid to liquid without the equilibration of three phases. The transition S + V → V was earlier denoted as evaporation by some authors (Kreulen and Schuiling, 1982) whereas the transition S + L → L was denoted as final melting (Herskowitz and Kisch, 1984) or dissolution. The term sublimation is preferred here for both transitions as a distinction between liquid and vapor cannot be made by observation. In the more general case of CO_2-CH_4-N_2 inclusions, it cannot always be decided if the resulting fluid has the character of a liquid at the temperature of disappearance of the solid, even when this transition is preceded by partial homogenization to liquid or vapor.

The behavior of fluid inclusions can be typified with the help of a classification model (van den Kerkhof, 1988a, 1988b, 1990), based on a distinction in two main types: (1) H-type inclusions characterized by homogenization (T_h) as the final phase transition, preceded by incipient and final melting (T_i and T_m respectively): S + V or S + L → S + L + V → L + V → L or V and (2) S-type inclusions characterized by sublimation (T_s), preceded by partial homogenization (T_{hs}): S + L + V → S + V or S + L → V or L. The sequence of phase transitions is fixed for both groups. The groups can be further typified according to the total number of phase transitions between −160 and +35 °C (types H1-5 and S1-4) and to the resulting phase: liquid, vapor, or critical [e.g., types H2(L), H2(V), H2(C)].

In our samples four types of fluid inclusions could be distinguished according to this classification: S2(L), H2(L,C), H1(L,C), and H1(V). These types generally do not show any textural distinctions, except for a portion of the H1(V) inclusions, which also include the irregular decrepitated inclusions. The decrepitated inclusions do not show any phase transition and are not further considered. S2(L) and H2(L,C) inclusions were most frequently observed; the other 2 types are probably the result of partial decrepitation.

The type S2(L) inclusions are most common among the methane-rich inclusions. Two examples of the phase behavior are shown in Figure 3a. Partial homogenization (T_{hs}) and sublimation (T_s) temperatures fall into two distinct groups: (1) samples (Ap79-5C and 7B) from the Silurian and Lower Devonian of the Delaware Water Gap–Stroudsburg area (terrane 1b) showing T_{hs} largely between −124 and −103 °C and T_s from −98 to −85 °C; (2) samples from the Pennsylvanian of the anthracite fields (Ap80-26, 33A, 49, 51, 56F, and 64) showing T_{hs} between −90 and −74.5 °C and T_s from −79 to −71.5 °C. In the only exception, sample Ap80-26 from the Bear Valley strip mine in the western middle anthracite field, shows somewhat lower T_{hs} temperatures of −92 to −84 °C.

In some inclusions of the S2(L) type, homogenization of the metastable (undercooled) liquid was observed in the absence of solid CO_2; the metastable T_{hm} temperatures were 3–5 °C higher than the stable T_{hs} temperatures of the same inclusion, which reflects the oversaturation of the undercooled liquid with CO_2.

The type H2(L,C) inclusions are less frequent than S2(L) inclusions. Examples of phase sequences are shown in Figure 3b. Melting temperatures (−97 to −72 °C) are in the same range as sublimation. However, homogenization temperatures (T_h) are up to 13 °C higher than melting of solid CO_2 (T_m) for the same inclusions. In a few cases homogenization was accompanied by critical phenomena (meniscus fading or meniscus efferverscence). The similarity of the T_m temperatures to the T_s temperatures of the type S2(L) inclusions from the same area indicate the similarity in composition of the fluids.

When type H1(L,C) inclusions are cooled, solid CO_2 does not nucleate even at temperatures as low as −180 °C. Homogenization (to the liquid phase or critical phase) is therefore the only phase transition that can be observed (Fig. 3c). T_h shows a narrow range between −87 and −81 °C, not far from the critical temperature of CH_4 (−82.6 °C). The absence of solid CO_2 at low temperatures indicates that compositions are between the eutectic composition and pure CH_4. However, the eutectic approximates the triple point of CH_4 (Davis et al., 1962), but optical restrictions may hinder the observation of the solid particle. It was found that solid CO_2 can be observed in CH_4-CO_2 inclusions containing more than about 3 mol% CO_2.

Type H1(V) inclusions show homogenization temper-

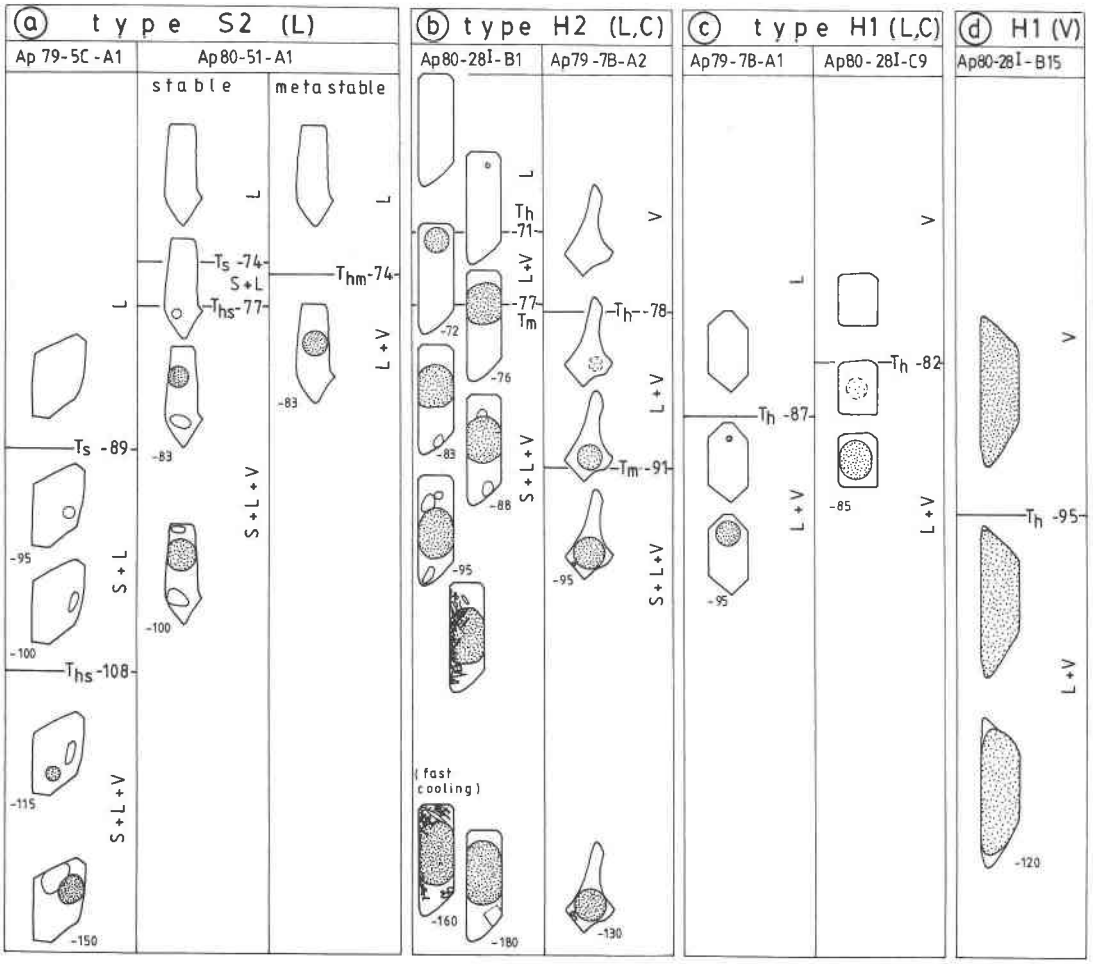

Fig. 3. Examples of phase sequences in CH_4-CO_2 inclusions observed in the temperature range from −160 to +35 °C. The stippled parts indicate the vapor phase. **(a)** Type S2(L) showing the phase sequence S + L + V → S + L → L for the stable phases and L + V → L for the metastable phases. The latter transition can only be observed for inclusions that show the nucleation of the bubble before the nucleation of solid CO_2 on cooling. **(b)** Type H2(L) characterized by the phase sequence S + L + V → L + V → L. Some inclusions show final critical homogenization [H2(C)]. **(c)** Type H1(L,C) showing only homogenization of liquid and vapor, and no nucleation of solid CO_2 on cooling to −180 °C. Some inclusions show critical homogenization around −82.6 °C (the critical temperature of methane). **(d)** Type H1(V) representing methane inclusions of low density with homogenizations to the vapor phase.

atures between −100 and −94 °C, significantly lower than for the H1(L,C) inclusions (Fig. 3d).

Raman analysis

Quantitative analysis of the gaseous inclusions were made by obtaining Raman spectra. The apparatus used is a Microdil-28 Raman microspectometer provided with a multichannel detector (Burke and Lustenhouwer, 1987).

Six samples were selected for Raman analysis:

Group 1a: Ap79-56 from the Lizard Creek member of the Shawangunk Formation (Silurian), Delaware Water Gap, New Jersey; Ap79-7B from the Oriskany Formation, Route 611 between Delaware Water Gap and Stroudsburg, Monroe County, Pennsylvania.

Group 2: Ap80-26 and 28I from the Bear Valley mine, western middle anthracite field, Northcumberland County, Pennsylvania (Shamokin 7½ min quadrangle); Ap80-51 from Sugar Noth near Wilkes Barre, northern anthracite field, Luzerne County, Pennsylvania (Wilkes-Barre west 7½ min quadrangle); Ap80-56F from interstate Route 81 near junction with Route 115 near Wilkes-Barre, northern anthracite field, Northcumberland County, Pennsylvania (Wilkes-Barre east 7½ min quadrangle).

The most important gases, detected in these samples, are CH_4 and CO_2 (up to 22 mol%); the amount of N_2 was less than 1.5 mol% in the samples from the Delaware Water Gap area and absent in the anthracite fields. Given the recorded presence of ammonium-bearing illites for

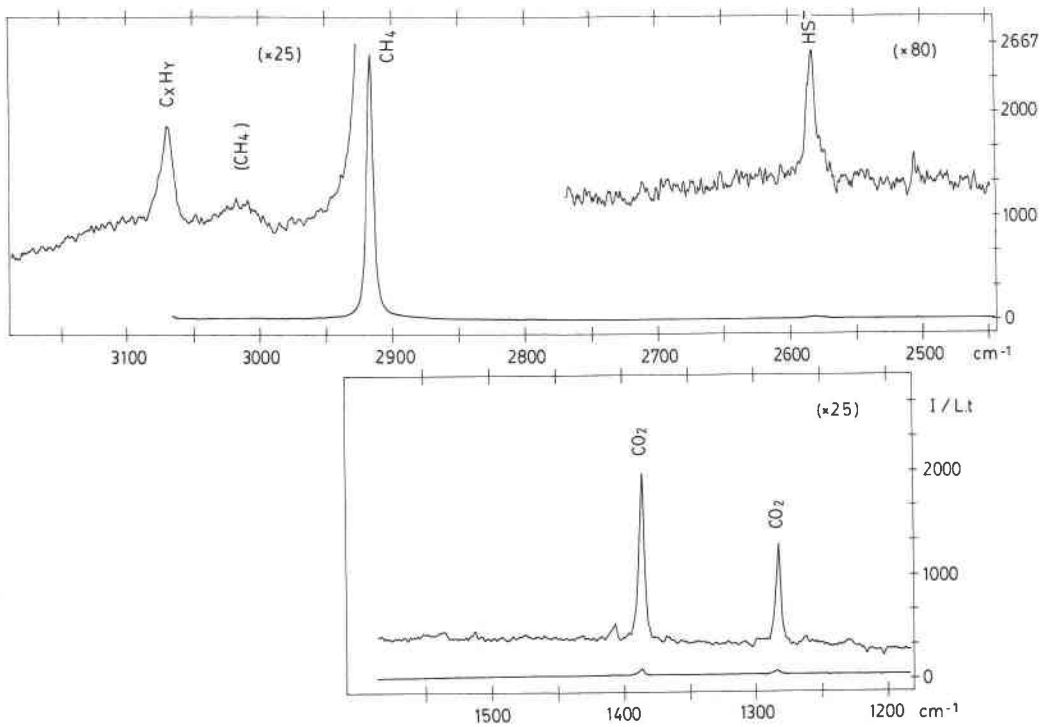

Fig. 4. Raman spectra recorded for one inclusion (Ap80-281-A1) for the compounds CH_4, HS^-, and CO_2. The peak at about 3069 cm^{-1} indicates the presence of higher hydrocarbons.

the anthracite fields (Juster et al., 1987), the low N_2 contents are remarkable.

The Raman spectrum of methane is characterized by a strong peak that shifts in position between 2913.5 and 2916.2 ± 0.6 cm^{-1} for most of the samples (from higher to lower density) and 1919.5 cm^{-1} for the inclusions of lowest density. From these values the maximum pressure in the inclusions at room temperature is interpreted to be about 0.5 kbar (van den Kerkhof, 1988a). The Raman spectrum of CO_2 consists of two peaks with the positions at 1280–1283 ± 0.8 cm^{-1} and 1383–1386 ± 0.8 cm^{-1} i.e., slightly below the theoretical values of 1285 and 1388 cm^{-1} for pure CO_2 at 1 atm. Calculations are made by using the latter peak of higher intensity. N_2 in the fluid inclusions shows a single peak around 2327–2329 ± 0.7 cm^{-1} (2331 cm^{-1} at 1 atm).

Small amounts of hydrogenated S (<1 mol%) could be detected in several samples. The peaks are situated in the range between 2576 and 2582 cm^{-1} corresponding to hydrogenated S in the ionic state (HS−) (Rosasco and Roedder, 1979; Bény et al., 1982; van den Kerkhof, 1988a).

A weak peak around 3069 cm^{-1} in sample Ap80-28 (Fig. 4) was earlier described by Guilhaumou (1982), and it is assumed to indicate the presence of aliphatic hydrocarbons or aromatic hydrocarbons, or both. These compounds indicate lower temperatures of formation as they will decompose above 250 °C. This finding agrees with trapping temperatures for the anthracite region indicated by microthermometry (see below).

The relative amounts (in molar proportions) of the gases were calculated from the peak integrals and by using the following relative Raman cross-sections (σ): CH_4 (8.9), CO_2 (1.21), N_2 (1), HS− (as for H_2S, 6.8). For the two compounds CH_4 and CO_2, the relative amounts can be calculated from the following expression which was deduced from the Placzek equation (Placzek, 1934; Dubessy, 1985; van den Kerkhof, 1988a):

$$N_{CO_2} = \frac{A_{CO_2} \cdot \sigma_{CH_4}}{A_{CH_4} \cdot \sigma_{CO_2}} \quad \text{and} \quad N_{CH_4} + N_{CO_2} = 100\%$$

where A = peak integral, σ = relative Raman scattering cross-section, and N = the number of molecules. The results are listed in Table 2.

In one inclusion, the formation of graphite in a gas inclusion was noticed during the analysis. It is assumed that the following reaction is initiated by the induction of the laser: $CO_2 + CH_4 \rightarrow 2C + 2H_2O$.

The gas bubbles of the aqueous inclusions were checked for their composition by Raman analysis. As the Raman activity of H_2O is extremely weak, it is not possible to do quantitative analysis on H_2O gas inclusions. However, qualitative indications on the CH_4 content of the gas bubble can be obtained by the detection of Raman spectra at comparable conditions (inclusion size and depth, laser power, etc.). It was found that the CH_4 content varies

TABLE 2. Microthermometric and Raman data

Number	Ty*		T_{hs}	T_{hm}	T_h		$T_{m/s}$	H_2O	CH_4	CO_2	N_2	HS^-	$\bar{V}$
(1) Delaware Water Gap area:													
Ap79-5C													
A1	S2	L	−108.2			S	−89.3	–	92.0	6.5	0.7	0.8	46
A4	S2	L	−107.7			S	−89.3	–	92.9	5.8	1.3		46
A6	H1	L			−81.4	—	—	+	94.5	4.3	1.2		72
—									92.4	7.3	0.3		
Ap79-7B													
A1	H1	L			−86.6	—	—	–	96.2	3.0	0.8		62
A2	H2	L/C			−77.5	M	−90.7	–	95.9	3.6	—	0.5	~80
A3	S2	L	−123.5			S	−95.8	–	95.4	3.8	0.8		41
A4	S2	L	−124.2			S	−95.8	–	96.3	2.9	—	0.8	41
(2) Pennsylvania anthracite fields:													
Ap80-26													
A1	S2	L	−84.1	−81.1		S	−76.4	–	85.1	14.9	—		58
Ap80-51													
A1	S2	L	−77.2	−74.4		S	−73.5	–	85.1	14.9	—	—	62
A4	S2	L	−82.4	−78.0		S	−73.9	–	84.7	15.3	—		60
A7	H2	L			−67.1	M	−72.8	–	79.0	21.0	—		64
—									85.7	14.3			
Ap80-56F													
A1	S2	L	−88.4	−85.1		S	−78.4	–	91.9	8.9	—		57
A3	S2	L	−90.4	−86.5		S	−78.4	–	86.1	13.9			54
A5	S2	L	−88.1	−85.1		S	−79.1	–	**	**			56
Ap80-28I													
A1	H2	L			−70.8	M	−77.4	–	89.7	9.5	—	0.7	72
B1	H2	L			−70.8	M	−76.9	–	89.3	10.7	—	—	70
B15	H1	V			−94.7	—	—	–	100	—	—		281
C1	H2	L			−70.6	M	−76.9	–	77.7	22.3	—	—	69
C9	H1	C			−82.0	—	—	–	99.5	—	—	0.5	99
C10	H1	V			−96.3	—	—	–	100	—	—	—	303

Note: The results for some selected fluid inclusions: only Raman-analyzed inclusions are listed (most of the data, used for the interpretation of trapping *P-T* conditions, are not listed).

* Ty = type of fluid inclusion (see text); T_{hs}, T_{hm}, T_h, $T_{m/s}$ (see text for definitions). All temperatures are given in Celcius; H_2O = water observed optically; gas compositions are measured by Raman analysis and expressed in mol%.

** Denotes the formation of graphite during Raman analysis by induction of the laser beam according to the reaction $CO_2 + CH_4 \rightarrow 2C + 2H_2O$. Estimated molar volumes ($\bar{V}$) are given in cm³/mol.

strongly: some bubbles show high intensities for the CH_4 line, while others show only a weak or no CH_4 signal. It can be assumed that the aqueous inclusions with highest CH_4 contents were also saturated with methane at the trapping conditions. A rough indication of the maximum CH_4 content can be made from the degree of filling (0.8–0.9) and the molar volumes of the H_2O (18 cm³/mol) and gas phases (>100 cm³/mol). The total molar volume of the inclusions is about 20–22.5 cm³/mol. It can be assumed that the maximum CH_4 content is about 2–4.3 mol%. Even these small amounts of CH_4 in aqueous inclusions have important implications for the interpretation of trapping temperatures (see below). On the other hand, the CH_4 contents of aqueous inclusions in veins without methane-rich inclusions are very low; no CH_4 was found in aqueous inclusions in a quartz vein from the Martinsburg Formation, and very little in two from the underlying Ordovician Epler Limestone. These inclusions show low homogenization temperatures of respectively 96–127 °C and 105–137 °C.

THE MOLAR VOLUME OF GASEOUS INCLUSIONS

The gaseous inclusions can be considered as binary mixtures between CH_4 and CO_2 as the other compounds are only accessory. The topology of the multiphase region of the system CO_2-CH_4 (Burruss, 1981; van den Kerkhof, 1988a, 1990) was established from Donnely and Katz (1953), Davis et al. (1962), Arai et al. (1971), Hwang et al. (1976), and Mraw et al. (1978). An equation of state valid for the low temperature region was given by Heyen et al. (1982). Several other equations were checked by Herskowitz and Kisch (1984) who proposed a model for the region for which "$T_h < T_m$" (type S2), based on the Peng-Robinson equation (Fig. 5).

The diversity of phase behavior and the combined microthermometric and Raman data give rise to two distinct generations of fluid inclusions: (1) S2(L) and H2(L) inclusions showing a wide volumetric variation: the molar volume varies between 41 and 62 cm³/mol for the type S2 inclusions and between 62 and 80 cm³/mol for type H2 inclusions (Fig. 5). The good correlation between molar volume and composition is remarkable; higher CO_2 contents occur for inclusions of higher molar volume (lower density). (2) H1(L,C) and H1(V) inclusions with molar volumes up to about 1000 cm³/mol. There is a tendency for lower CO_2 contents with higher molar volumes: inclusions of highest molar volume consist of pure CH_4.

Evaluation of microthermometry on aqueous inclusions in the quartz veins; conditions of trapping

The aqueous inclusions on which the melting behavior of ice was observed showed final melting temperatures ranging from approximately −8 to −1 °C, corresponding to equivalent NaCl contents of about 12 to 2 wt% respectively. Since the differences in the slope of the isochores caused by variations in salinity in the range of 0–10 wt% NaCl are minor, their effect on the intersection temperature with the isochores of the methane-rich fluids in the pressure range of interest are negligible. In view of this, and of the scatter in the homogenization temperatures, observation of the melting behavior of ice in most of these aqueous fluid inclusions was dispensed with.

Assumption of pure H_2O

The predominant $T_{h,aq.}$ values measured in samples Ap79-5C and 7B from the Silurian and Delaware Water Gap–Stroudsburg area lie at 180 °C to 230 °C, but several much higher temperatures were found (Fig. 2). The corresponding densities (for pure H_2O) are 0.83–0.88 g/cm³ ($\bar{V}$ = 20.5–21.7 cm³/mol) (Fisher, 1976). Isochores for pure H_2O with these densities would intersect the isochores for methane-rich inclusions with T_h = −110 °C to −103 °C, the most common in these samples, as calculated using the Peng-Robinson equation of state (Herskowitz and Kisch, 1984), in the P-T range 1.8 kbar, 300 °C to 2.4 kbar, 320 °C (for $T_{h,aq.}$ = 180 °C) to 2.2 kbar, 360 °C to 2.8 kbar, 410 °C (for $T_{h,aq.}$ = 230 °C). For the aqueous inclusions in samples from the Pennsylvanian anthracite fields, the predominant $T_{h,aq.}$ values are slightly higher, ranging from 195 to 245 °C. Intersection of the pure H_2O isochores for these temperatures with the isochores of the most common methane-rich fluid inclusions, with T_h = −90.5 to −77 °C (or $\bar{V}$ = 52–64 cm³/mol), as calculated using the same method, yields pressures and temperatures in the range 0.95 kbar, 255 °C to 1.5 kbar, 290 °C (for $T_{h,aq.}$ = 195 °C) to 1.1 kbar, 320 °C to 1.7 kbar, 360 °C (for $T_{h,aq.}$ = 245 °C).

Assumption of methane-saturated H_2O

As mentioned above, CH_4 was detected in the bubbles of H_2O inclusions. However, quantitative analysis of H_2O-CH_4 inclusions is not possible by Raman analysis. Addition of CH_4 to H_2O inclusions results in a shift of H_2O isochores to lower temperatures compared to pure H_2O (Hanor, 1980; Burruss, 1989). The H_2O-CH_4 isochores should start at the interception of the CH_4-CO_2 isochores, lines of constant $T_{h,aq.}$, and an appropriate saturation curve (Price, 1979) (Fig. 6). Hanor (1980) stated that, if the homogenization temperatures took place at relatively high pressures, the pressure correction would be smaller by some 60 °C for every kilobar increase in pressure at T_h.

The uncertainty of CH_4 contents of the aqueous inclusions can be evaded by assuming that the aqueous and methane-rich fluids were in equilibrium at the time of their trapping. This assumption of simultaneous entrapment is supported by the similarity in shape, distribution, and mode of occurrence of aqueous and methane-rich inclusions. Consequently, the aqueous inclusions must have been CH_4 saturated at the time of trapping. Since any saturated fluid will exsolve its solute upon cooling (unless cooling is accompanied by an increase in pressure—a rare combination in constant-volume systems), a CH_4-rich gas phase should have exsolved upon the inception of cooling from the trapping temperature. The $T_{h,aq.}$ thus measured must represent the real trapping temperature, without any need for applying a pressure correction, and the $T_{h,aq.}$ intercepts on the isochores of the methane-rich inclusions approximate the P-T conditions of trapping (Fig. 6). If the aqueous fluids were CH_4 saturated upon trapping, accordingly the methane-rich fluids should have been H_2O saturated. However, no exsolution of an aqueous phase was observed in the latter, probably because a minor aqueous phase only wets the wall of the inclusion and forms a very thin film, which is almost impossible to observe. One might have expected to observe clathrate melting upon heating these inclusions after cooling to −30 °C, but since clathrate contains much more H_2O than CH_4, the quantities of clathrate will be very small, and similarly not observable.

In the case of the Delaware Water Gap samples, the

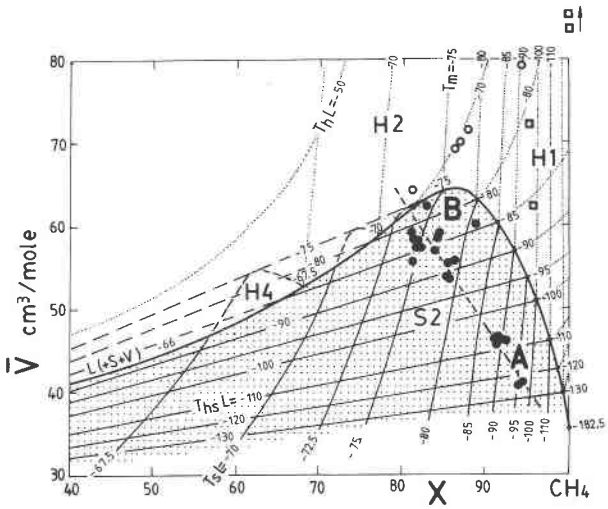

Fig. 5. $\bar{V}X$ diagram of the system CO_2-CH_4 for molar volumes between 30 and 80 cm³/mol (after Herskowitz and Kisch, 1984). The three-phase curve L(+ S + V) delimits the regions characterized by sublimation (stippled) and homogenization (open) (see text). A selection of isotherms (°C) marking partial homogenization (T_{hs}L) and sublimation (CO_2 dissolution) (T_sL) temperatures is shown for the S-type inclusions; the isotherms marking homogenization (T_hL) and melting (T_m) for the H-type inclusions are tentative. Plotted are the microthermometry data of the type S2 inclusions (black dots), some H2 (open dots) and H1 inclusions (squares) from the Silurian-Devonian of the Delaware Water Gap area (A) and from the anthracite region of east Pennsylvania (B).

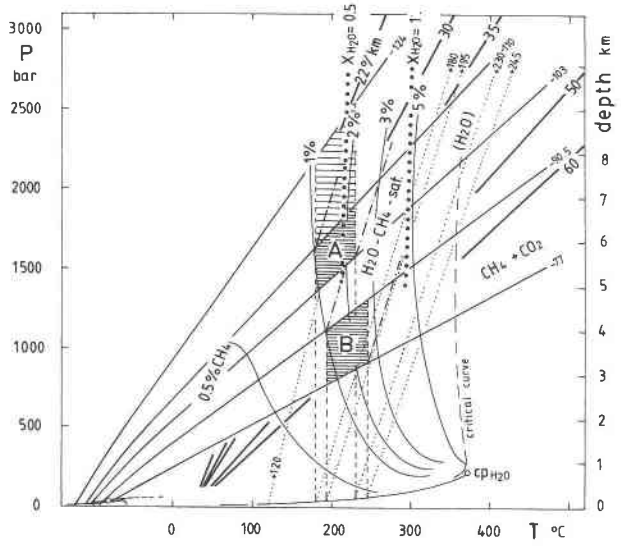

Fig. 6. The estimation of fluid trapping P-T conditions from isochores. The isochores for the CH_4-CO_2 inclusions (solid lines) are calculated from the Peng-Robinson equation of state (Herskowitz and Kisch, 1984); isochores for pure H_2O (dotted lines) are taken from Fisher (1976). The assumption of CH_4 saturated H_2O at trapping implies forming temperatures equal to $T_{h,aq.}$ (dashed lines). The isochores for the aqueous inclusions containing CH_4 (H_2O-CH_4-sat.) are shifted to lower temperatures compared to the isochores for pure H_2O with the same molar volume. The estimated trapping pressures for the Silurian-Devonian of the Delaware Water Gap area (A) are significantly higher than for the anthracite region of east Pennsylvania (B). The saturation curves for 5, 3, 2, 1, and 0.5% CH_4 are extrapolated after the data of Price (1979). Also shown are the geothermal gradients corresponding to A (22 and 30 °C/km) and B (50 and 60 °C/km). The heavily dotted lines show the equilibrium of the reaction kaolinite + quartz ⇌ pyrophyllite + H_2O at $X_{H_2O} = 1$ and $X_{H_2O} = 0.5$.

intercepts of the isochores of the methane-rich fluids (T_h = −110 to −103 °C) with 180 and 230 °C correspond to pressures of 1.3–1.6 kbar for $T_{h,aq.}$ = 180 °C and 1.6–1.9 kbar for $T_{h,aq.}$ = 230 °C. The occasional higher T_h values measured in some of the aqueous inclusions are considered to represent heterogeneous trapping of H_2O-CH_4 mixtures. For the denser CH_4-rich inclusions with T_h = −124 °C in sample Ap79-7B, the assumption of saturation of the aqueous fluids with CH_4 implies even higher pressures of trapping, the 180 and 230 °C intercepts on the isochore corresponding to pressures of respectively 2.2 and 2.5 kbar. If pressures are taken to be lithostatic, these correspond to burial depths of 8–9 km and give a mean geothermal gradient of about 180 °C/8–9 km or 22–20 °C/km, a rather normal continental and metamorphic thermal gradient. These temperatures are corroborated by the much lower homogenization temperatures $T_{h,aq.}$ of methane-poor aqueous fluid inclusions in nearby samples from the Ordovician underlying the Taconic unconformity of the Delaware Water Gap in which no methane-rich inclusions were found. $T_{h,aq.}$ values of 96–127 °C were measured on aqueous inclusions in the Martinsburg Formation (no methane detected) and 105–136 °C (115–137 °C in all except one of 25 inclusions) on aqueous inclusions in the Epler Limestone (very little methane detected). Assuming these fluids to be pure H_2O, the isochore for the mean $T_{h,aq.}$ value at ~120 °C intersects the isochores T_h = −103 to −110 °C of the methane-rich fluids in samples Ap79-5C and 7B at 180 °C, 1.3 kbar to 200 °C, 1.7 kbar (Fig. 6), in good agreement with the P-T box A found on the assumption of methane saturation of the aqueous inclusions in these samples.

Slightly higher homogenization temperatures of 132–138 °C (nine inclusions) were measured on aqueous inclusions in a quartz vein from the Silurian in which no methane-rich inclusions were found; the unusually low temperatures of final ice melting (−14 to −11 °C) in these aqueous fluids attest to their high salinity, which explains the low solubility of methane (Hanor, 1980, Fig. 2).

If saturation of aqueous solutions with CH_4 is similarly assumed for the samples from the Pennsylvanian anthracite, the intercepts of the isochores of the methane-rich fluids (T_h = −90.5 to −77 °C) with 195 and 245 °C correspond to pressures of 0.8–1.1 kbar for $T_{h,aq.}$ = 195 °C, and 0.9–1.3 kbar for $T_{h,aq.}$ = 245 °C. Even if the denser inclusions (~53 cm³/mol) with the lower homogenization temperatures around −90 °C are regarded as most closely approximating the original trapping conditions (and the maxima of the above pressure ranges adopted accordingly), these values would imply much higher geothermal gradients of about 170 °C/3.0 km or 220 °C/4.5 km, or 45–50 °C/km.

The assumption that $T_{h,aq.}$ represents trapping temperatures requires that the pressures ($P_{h,aq.}$) in the fluid inclusions at $T_{h,aq.}$ should equal the trapping pressures. The frequent observation of decrepitation of the inclusions, mostly shortly after homogenization, may indicate the high internal pressures. Several inclusions decrepitated at temperatures lower than those of homogenization.

The difference in burial depth of 3 to 4 km deduced from the inclusions from the Silurian and Devonian of the Delaware Water Gap–Stroudsburg area agrees with published data on the combined thickness of the Devonian and Mississippian in the Valley and Ridge province of eastern Pennsylvania, which totals about 3300 m—the Silurian having an additional thickness of 900 m (King, 1977, Fig. 35).

The high geothermal gradients found for the Pennsylvanian anthracite fields agree with other evidence for high-temperature (low P-T) metamorphic gradients in the anthracite fields, such as the almost ubiquitous association of pyrophyllite with illite that has not yet become sufficiently coarse to be considered anchimetamorphic crystallinities (cf. Kisch, 1987). Use of the less dense inclusions with T_h values of −80 °C to −75 °C would imply even higher geothermal gradients.

The occurrence of pyrophyllite in underclays of the an-

thracites (Hosterman et al., 1970; see also Kisch, 1987, p. 263) is compatible with the above temperature range. The univariant equilibrium kaolinite + quartz ⇋ pyrophyllite + H_2O is in equilibrium at 295 and 310 °C at fluid pressures of 1.5 and 4.0 kbar (Reed and Hemley, 1966; Frey, 1987, Fig. 2.9). Haas and Holdaway (1973) consider the temperatures of 325 to 375 °C of Thompson (1970) "a little high." However, these equilibrium temperatures are depressed at increased X_{CO_2} (or decreased X_{H_2O}) at constant total fluid pressure by about 17 °C/0.1 X_{CO_2}, and for instance are 215 and 225 °C at $X_{CO_2} = 0.5$ at total fluid pressures of 1.5 and 4.0 kbar (Fig. 6). The appearance of pyrophyllite together with kaolinite at relatively low temperatures can thus be accounted for by the high methane and CO_2 contents of the fluids.

The temperatures of 195–245 °C found in the anthracite fields correspond to the lower part of the temperature range of the anchimetamorphic zone (cf. Kisch, 1987). The occurrence of poorly evolved diagenetic illite crystallites in the anthracite fields therefore requires an explanation. Two possibilities may be suggested, which may have acted in combination: (1) The postkinematic occurrence of the heating or its brief duration, which have been shown in other areas to result in a lag of the evolution of illite crystallinity after that of other parameters of very low-grade metamorphism (cf. Kisch, 1987), and (2) A low K^+/H^+ ratio in the fluid due to the high organic matter content in the coal measures, and partly evident from the persistence of kaolinite, and the widespread occurrence of the K-poor phyllosilicates, pyrophyllite and ammonium illite. Such a potassium deficiency could inhibit the evolution of illite to muscovite (Kubler, 1967, p. 390–391; Kisch, 1983, p. 351–352).

It is concluded that very low-grade metamorphism of the Delaware Water Gap–Stroudsburg area (180–230 °C, 1.3–1.9 kbar) and the Pennsylvanian coal measures (195–245 °C, 0.8–1.3 kbar) is reflected by fluid inclusions that formed from immiscible fluids in the system H_2O ($\pm$NaCl)-CH_4-CO_2. The metamorphic temperatures found by the interpretation of microthermometry and Raman data are mostly in agreement with earlier results by other methods (anthracite ranks, pyrophyllite stability, illite crystallinity, stratigraphic data, conodont alteration indices, slaty cleavage). The fluid inclusion study appeared to be most suitable to reveal more accurate data on metamorphic pressures. However, illite crystallinities sometimes indicate much lower temperatures of rock formation and these data need further evaluation.

Acknowledgments

Facilities for the laser Raman microprobe were provided by the Free University in Amsterdam and by NWO (Netherlands Organization for Scientific Research). E.A.J. Burke is kindly acknowledged for assistance during Raman analysis. A portion of the microthermometric measurements was carried out by H. Kisch using facilities kindly made available by Lincoln Hollister at the Department of Geological and Geophysical Sciences, Princeton University. The work of A.M. van den Kerkhof, as a part of a Ph.D. and postdoctoral study, was subsidized by NWO. We wish to thank J. Touret at the Free University (Amsterdam) for his helpful advice. The referees P.E. Brown, R.C. Burruss, and W.T. Parry are thanked for their constructive reviews, which improved the clarity of the manuscript.

References cited

Arai, Y., Kaminishi, G., and Saito, S. (1971) The experimental determination of the PVTX-relations for the carbon dioxide–nitrogen and the carbon dioxide–methane systems. Journal Chemical Engineering Japan, 4, 113–122.

Bény, C., Guilhaumou, N., and Touray, J.-C. (1982) Native sulphur-bearing fluid inclusions in the CO_2-H_2S-S system—microthermometry and Raman microprobe (MOLE®) analysis—thermochemical interpretations. Chemical Geology, 37, 113–127.

Beutner, E.C. (1978) Slaty cleavage and related strain in Martinsburg slate, Delaware Water Gap, New Jersey. American Journal of Science, 278, 1–23.

Beutner, E.C., and Diegel, F.A. (1985) Determination of fold kinematics from syntectonic fibers in pressure shadows, Martinsburg slate, New Jersey. American Journal of Science, 285, 16–50.

Burke, E.A.J., and Lustenhouwer, W.J. (1987) The application of a multichannel laser Raman microprobe (Microdil-28®) to the analysis of fluid inclusions. Chemical Geology, 61, 11–17.

Burruss, R.C. (1981) Analysis of fluid inclusions: Phase equilibria at constant volume. American Journal of Science, 281, 1104–1126.

Burruss, R.C. (1989) Paleotemperatures from fluid inclusions: Advances in theory and technique. In N.D. Naeser and T.H. McCulloh, Eds., Thermal history of sedimentary basins: Methods and case histories, p. 119–131. Springer-Verlag, New York.

Davis, J.A., Rodewald, N., and Kurata, F. (1962) Solid-liquid-vapor phase behavior of the methane–carbon dioxide system. American Institute of Chemical Engineers Journal, 8-4, 537–539.

Donnely, H.G., and Katz, D.L. (1953) Phase equilibria in the carbon dioxide–methane system. Industrial and Engineering Chemistry, 46, 511–517.

Drake, A.A. (1969) Precambrian and lower Paleozoic geology of the Delaware Valley, New Jersey–Pennsylvania (Field trip no. 1-A). In S. Subitzky, Ed., Geology of selected areas in New Jersey and Pennsylvania and guidebook for excursions, p. 51–131. Rutgers University Press, New Brunswick, New Jersey.

Dubessy, J. (1985) Contribution à l'étude des interactions entre paléofluides et minéraux à partir de l'étude des inclusions fluides par microspectrométrie Raman—Conséquences métallogéniques, 198 p. Ph.D. thesis, Institut National Polytechnique de Lorraine, Nancy.

Epstein, J.B., and Epstein, A.G. (1969) Geology of the Valley and Ridge province between Delaware Water Gap and Lehigh Gap, Pennsylvania. In S. Subitzky, Ed., Geology of selected areas in New Jersey and Pennsylvania and guidebook for excursions, p. 132–205. Rutgers University Press, New Brunswick, New Jersey.

Epstein, A.G., Epstein, J.B., and Harris, L.D. (1977) Conodont alteration—an index to organic metamorphism. U.S. Geological Survey Professional Paper 995, 27 p.

Fisher, J.R. (1976) The volumetric properties of H_2O—a graphical portrayal. Journal Research U.S. Geological Survey, 4, 189–193.

Frey, M. (1987) Very low-grade metamorphism of clastic sedimentary rocks. In M. Frey, Ed., Low temperature metamorphism, p. 9–58. Blackie and Son, Glasgow.

Groshong, R.H. (1976) Strain and pressure solution in the Martinsburg slate, Delaware Water Gap, New Jersey. American Journal of Science, 276, 1131–1146.

Guilhaumou, N. (1982) Analyse ponctuelle des inclusions fluides par microsonde moléculaire à laser (MOLE®) et microthermométrie. Travaux du Laboratoire de Géologie, 14, 78 p. Presses de l'École Normale Supérieure, Paris.

Haas, H., and Holdaway, M.J. (1973) Equilibria in the system Al_2O_3-SiO_2-H_2O involving the stability limits of pyrophyllite, and thermodynamic data of pyrophyllite. American Journal of Science, 273, 449–464.

Hanor, J.S. (1980) Dissolved methane in sedimentary brines: Potential

effect on the PVT properties of fluid inclusions. Economic Geology, 75, 603–617.

Harris, A.G., Harris, L.D., and Epstein, J.B. (1978) Oil and gas data from Paleozoic rocks in the Appalachian basin: Maps for assessing hydrocarbon potential and thermal maturity (conodont color alteration isograds and overburden isopachs). U.S. Geological Survey Miscellaneous Investigations Series, Map 1-917-E, 4 sheets.

Herskowitz, M., and Kisch, H.J. (1984) An algorithm for finding composition, molar volume and isochores of CO_2-CH_4 fluid inclusions from T_h and T_{fm} (for $T_h < T_{fm}$). Geochimica et Cosmochimica Acta, 48, 1581–1587.

Heyen, G., Ramboz, C., and Dubessy, J. (1982) Simulation des équilibres de phases dans le système CO_2-CH_4 en dessous de 50 °C et de 100 bar. Application aux inclusions fluides. Comptes Rendus de l'Académie des Sciences de Paris, t. 294, série II, 203–206.

Holeywell, R. C., and Tullis, T.E. (1975) Mineral reorientation and slaty cleavage in the Martinsburg Formation, Lehigh Gap, Pennsylvania. Geological Society of America Bulletin, 86, 1296–1304.

Hosterman, J.W., Wood, G.H., and Bergin, M.J. (1970) Mineralogy of underclays in the Pennsylvania anthracite region. U.S. Geological Survey Professional Paper 700-C, C89–C97.

Hwang, S.-C., Lin, H.-M., Chappelear, P.S., and Kobayashi, R. (1976) Dew point study in the vapor–liquid region of the methane–carbon dioxide system. Journal of Chemical and Engineering Data, 21-4, 493–497.

Juster, T.C., Brown, P.E., and Bailey, S.W. (1987) NH_4-bearing illite in very low grade metamorphic rocks associated with coal, northeastern Pennsylvania. American Mineralogist, 72, 555–565.

Kerkhof, A.M. van den (1988a) The system CO_2-CH_4-N_2 in fluid inclusions: Theoretical modelling and geological applications, 206 p. Ph.D. thesis, Free University, Amsterdam.

Kerkhof, A.M. van den (1988b) Phase transitions and molar volumes of CO_2-CH_4-N_2 inclusions. Bulletin de Minéralogie, 111, 257–266.

Kerkhof, A.M. van den (1990) Isochoric phase diagrams in the systems CO_2-CH_4 and CO_2-N_2: Application to fluid inclusions. Geochimica et Cosmochimica Acta, 54, 621–629.

King, Ph.H. (1977) The evolution of North America (revised edition), 197 p. Princeton University Press, Princeton, New Jersey.

Kisch, H.J. (1980a) Incipient metamorphism of Cambro-Silurian clastic rocks from Jämtland Supergroup, central Scandinavian Caledonides, western Sweden: Illite crystallinity and "vitrinite" reflectance. In W.E.A. Phillips and M.R.W. Johnson, Eds., Deformation and metamorphism in the Caledonide Orogen. Journal of the Geological Society, London, 137, 271–288.

——— (1980b) Illite crystallinity and coal rank associated with lowest-grade metamorphism of the Taveyanne Greywacke in the Helvetic zone of the Swiss Alps. Eclogae geologicae Helvetiae, 73, 753–777.

——— (1983) Mineralogy and petrology of burial diagenesis (burial metamorphism) and incipient metamorphism in clastic rocks. In G. Larsen and G.V. Chilingar, Eds., Diagenesis in sediments and sedimentary rocks, 2. p. 289–493. Elsevier, Amsterdam.

——— (1987) Correlation between indicators of very-low-grade metamorphism. In M. Frey, Ed., Low temperature metamorphism, p. 227–300. Blackie and Son, Glasgow.

Kreulen, R., and Schuiling, R.D. (1982) N_2-CH_4-CO_2 fluids during formation of the Dôme de l'Agout, France. Geochimica et Cosmochimica Acta, 46, 193–203.

Kubler, B. (1967) La cristallinité de l'illite et les zones tout à fait supérieures du métamorphisme. In Étages Tectoniques—Colloque de Neuchâtel, 18–21 April 1966, p. 105–122. A la Baconnière, Neuchâtel, Switzerland.

Kubler, B. (1968) Évaluation quantitative du métamorphisme par la cristallinité de l'illite. Bulletin Centre de Recherches de Pau—SNPA, 2, 385–397.

Lee, J.H., Peacor, D.R., Lewis, D.D., and Wintsch, R.P. (1986) Evidence for syntectonic crystallization for the mudstone to slate transition at Lehigh Gap, Pennsylvania, U.S.A. Journal of Structural Geology, 8, 767–780.

Maxwell, J.C. (1962) Origin of slaty and fracture cleavage in the Delaware Water Gap area, New Jersey and Pennsylvania. In A.E.J. Engel, H.L. James, and B.F. Leonard, Eds., Petrologic studies: A volume in honor of A.F. Buddington, p. 281–311. Geological Society of America, Boulder, Colorado.

Mraw, S.C., Hwang, S.-C., and Kobayashi, R. (1978) Vapor-liquid equilibrium of the CO_2-CH_4 system at low temperatures. Journal of Chemical Engineering Data, 23-2, 135–139.

Pichavant, M., Ramboz, C., and Weisbrod, A. (1982) Fluid immiscibility in natural processes: Use and misuse of fluid inclusions data. I: Phase equilibria analysis. Chemical Geology, 37, 1–28.

Placzek, G. (1934) Rayleigh-Streuung und Raman Effekt. In E. Marx, Ed., Handbuch der Radiologie, vol. 6, p. 205–374. Akademische Verlagsgesellschaft, Leipzig.

Poty, B., Leroy, J., and Jachimowicz, L. (1976) A new device for measuring temperatures under the microscope: The Chaixmeca microthermometry apparatus. Bulletin de la Société française de Minéralogie et de Cristallographie, 99, 182–186.

Price, L.C. (1979) Aqueous solubility of CH_4 at elevated pressures and temperatures. American Association of Petroleum Geologists Bulletin, 63, 1527–1533.

Reed, B.L., and Hemley, J.J. (1966) Occurrence of pyrophyllite in the Kekiktuk Conglomerate, Brooks Range, northeastern Alaska. U.S. Geological Survey Professional Paper 550-C, C162–C165.

Rosasco, G.J., and Roedder, E. (1979) Application of a new Raman microprobe spectrometer to nondestructive analysis of sulphate and other ions in individual phases in fluid inclusions in minerals. Geochimica et Cosmochimica Acta, 43, 1907–1915.

Thompson, A.B. (1970) A note on the kaolinite-pyrophyllite equilibrium. American Journal of Science, 268, 454–458.

Weaver, C.E. (1961) Clay minerals of the Ouachita structural belt and the adjacent foreland. In P.T. Flawn, P.B. King, and C.E. Weaver, Eds., The Ouachita belt, p. 147–160. University Texas Publication 6120, Austin, Texas.

MANUSCRIPT RECEIVED JUNE 23, 1989
MANUSCRIPT ACCEPTED NOVEMBER 7, 1990